Polymer Testing 93 (2021) 106964

Contents lists available at ScienceDirect

Polymer Testing

journal homepage: http://www.elsevier.com/locate/polytest

Quasi-static and high strain rate response of Kevlar reinforced thermoplastics

Hemant Chouhan [a,*], Neelanchali Asija Bhalla [a], Aswani Kumar Bandaru [b], Shishay Amare Gebremeskel [a], Naresh Bhatnagar [a]

[a] Department of Mechanical Engineering, Indian Institute of Technology Delhi, New Delhi, India
[b] Marie Skłodowska-Curie Career-FIT Fellow, Irish Centre for Composites Research (IComp), School of Engineering, University of Limerick, Ireland

ARTICLE INFO

Keywords:
Kevlar
Thermoplastic matrices
Quasi-static
High strain rate
Failure mechanisms

ABSTRACT

The present study deals with the quasi-static and high strain rate characterization of Kevlar-129 based thermoplastic composites. Two different thermoplastic matrices, namely, Polypropylene (PP) and Polyetherimide (PEI) were used to manufacture composite laminates. Quasi-static compression tests were performed at strain rates of 0.041 s^{-1} and 0.045 s^{-1}. High strain rate tests were performed using a split Hopkinson pressure bar apparatus within the strain rates ranging from 2548 s^{-1} to 4379 s^{-1}. Stress-strain relations reveals the rate-sensitive behaviour of composites. Kevlar/PP (K-PP) showed higher peak stress under quasi-static loading as compared to the high strain rate test. Comparable peak stresses were revealed under quasi-static and high strain rate loading for Kevlar/PEI (K-PEI) composite. Also, high strain rate compression properties such as peak stress, peak strain and toughness of K-PP were 25%, 27% and 6% higher than that of the K-PEI composite. The failure mechanisms of both the composites were characterized through macroscopic and scanning electron microscopy. K-PP failed majorly due to matrix crush and fibre failure while K-PEI failed due to shear cracking. Damage study reveals that a single fibre based composite system can be tailored to act as an energy-absorbing or dissipating material system by varying the thermoplastic matrix materials.

1. Introduction

Fibre reinforced plastic (FRP) composites have emerged as a new class of materials over the last few decades for a wide variety of structural applications like bicycle frame, automobile, aerospace, buildings, marine and armor. The primary reason behind the widespread use of FRPs is their high specific strength and stiffness, coupled with superior corrosion resistance and efficient uses in competitive designs. Many applications like aerospace, protective structures and marine applications demand higher impact resistance as they are subject to high-velocity impact load and explosions during their service life.

The rate of loading plays a significant role in deciding the mechanical properties of a material. Rate of loading affects the deformation/damage behaviour of a material, governed by different mechanisms at different strain rates dictated by the speed of impacting projectile. The damage of a composite material as an outcome of high velocity projectile impact can be either ductile fracture or brittle fracture, depending on the constituents of the composites. Quasi-static characterization had been the preferred choice due to the availability of various standards to perform the tests under negligible inertial effects at a slow rate of loading. The response of the material changes with an increase in the rate of loading [1]. Under high strain rate loading conditions, the elastic-plastic wave-propagation effect becomes critical in the material. Since inertial effects come into action along with the adiabatic heating of the material. Adiabatic heating results in variation in the deformation/damage behaviour and associated with damage response is material strength characteristics. FRPs are extensively used for high strain rate applications in ballistics, aerospace and naval applications. Therefore, the study of composite systems meant for such applications is essential to reveal the nature of material behaviour as a function of the rate of loading.

Several studies were carried out to reveal the rate-dependent behaviour of neat polymers [2–4] as well as individual fibres [5–10]. Nakai and Yokoyama [2] studied six different polymers, including polypropylene (PP), under quasi-static and high strain rate loading and reported that polymers exhibit intrinsic dynamic viscoelastic–plastic behaviour. Omar et al. [3] studied three polymers, including PP within

* Corresponding author.
E-mail address: hchouhan@mech.iitd.ac.in (H. Chouhan).

https://doi.org/10.1016/j.polymertesting.2020.106964
Received 15 August 2020; Received in revised form 30 October 2020; Accepted 16 November 2020
Available online 20 November 2020

the strain rate range of 10^{-2} s^{-1} to 1100 s^{-1} and reported an increase in the yield strength by 150%. Mutter [4] studied neat Polyetherimide (PEI) under static and high strain rate loading conditions.Based on the macro-mechanical response, the quasi-static stress-strain curve of PEI was classified into four distinct regimes. A significant change in stress as a function of strain rate was noted with thermal softening resulting in lower stress under quasi-static loading [4].

Similarly, individual fibre and bundles have also been studied to reveal the rate-dependent behaviour of fibres. Lim et al. [5] measured small axial strain (5%) of Kevlar 129 fibre using a non-contact laser--based technique in a miniaturized tension Kolsky bar for a constant strain rate of 1500 s^{-1}. It was reported that with an increase in the gauge length, ultimate strength and strain decreases while modulus increases. Tan et al. [6] characterized quasi-static and rate-dependent mechanical properties of aramid yarns. They reported that strength increases as a function of the rate of tensile loading in the range of 0.0003 s^{-1} to 400 s^{-1}. Wang and Xia [9] studied the tensile behaviour of Kevlar 49 fibre bundles under quasi-static and dynamic strain rates of loading. Significant growth in modulus with nominal growth in strength, strain and toughness was observed with an increase in the strain rate. Zhang et al. [11] reported Young's modulus and tensile strength increment as the tensile strain rate increased from 25 to 50 s^{-1} for Kevlar-29 and Kevlar-49, respectively. However, further increment in the strain rate till 200 s^{-1} resulted in the decrement of properties [12,13].

Composites derived from above mentioned individual constituents have also been studied for the rate effect on their mechanical behaviour. Woo and Kim [14] studied the progress of failure in Kevlar woven composite under high strain rate loading using acoustic emission technique. An increased modulus, strength and toughness with decreasing strain as a function of rising strain rate was reported within the compressive strain rate range of 1182–1460 s^{-1}. Damage studies revealed that failure primarily consisted of matrix fracture, fibre–matrix debonding, cracking and some fibre breakages due to the impact force. Woo et al. [15] extended their work on studying Kevlar/carbon hybrid composite and revealed that strength increases as a function of strain rate. Though the growth pattern of the hybrid composite was identical to the neat Kevlar composite, the presence of carbon completely changed the damage behaviour of the composite. The hybrid woven Kevlar/-carbon composite failed due to matrix fracture, pull-out of the Kevlar and carbon fibres, interfacial failure and debonding. The brittle rupture of carbon fibres and fibrillation of Kevlar fibres was due to the compressive stress acting perpendicular to the fibre were the important findings of their study. Viswanathan et al. [16] worked on Kevlar/Polyethylene composite having a high fibre volume fraction of 85%. They concluded that yield stress increases and yield strain decrease at high strain rates in both the in-plane and in the thickness directions as compared to the quasi-static properties. Shaker et al. [17] studied the rate-dependent behaviour of Aramid and ultra-high molecular weight polyethylene fibre reinforced composites and reported that Uni-directional (UD) aramid-reinforced composite possesses the highest out-of-plane compression properties. However, energy absorption was noted highest for the hybrid composites.

Similar studies are available in the literature focusing on the high strain rate compressive behaviour of different composites to reveal the fact that the strength properties vary with rising strain rates [18–20, 30].. The literature available on comparison of the quasi-static and high strain rate testing generally uses different dimensions of a specimen. Whereas quasi-static testing demands international standards like ASTM D6641 to follow the specimen's aspect ratio. High strain rate testing, on the other hand, requires specimen aspect ratio resulting in negligible inertial effects given by specimen having an aspect ratio of $\sqrt{0.75\upsilon}$, where $\upsilon$is the material's Poisson's ratio [21]. Therefore, there is a strong need to reveal the effect of the rate of loading on identically dimensioned Kevlar-thermoplastic composite specimens, as presented in the literature [1,19] for other fibre-based composite systems. However, not much literature is available on the comparison of quasi-static properties with high strain rate properties of identically dimensioned Kevlar-reinforced high-performance thermoplastic polymers like impact grade PP and PEI. Compared to thermosetting matrices, the use of thermoplastic matrix can further enhance the performance of composites due to their lower density and viscosity [22,23].

The objective of the present study was to characterize the behaviour of Kevlar reinforced thermoplastic composites under quasi-static and high strain rate compression loadings. Two different composites were manufactured using Kevlar 129 fabric with impact grade PP and PEI as matrices. Quasi-static compression tests at low strain rate and dynamic compression tests at high strain rates were performed on these composites using split Hopkinson pressure bar (SHPB) set-up. The high strain rate properties of K-PP and K-PEI were compared in terms of peak stress, peak strain and toughness. Dynamic failure mechanisms were analysed at both macroscopic and microscopic scales.

2. Experiments

2.1. Materials

Kevlar 129 (K129) fabric with a two-dimensional plain woven structure (Grade: 802F, Make: DuPont) was used as reinforcement. High impact Polypropylene (Grade: Repol CO15EG, Make: Reliance Polymers) and Polyetherimide (Grade: Ultem 1000, Make: Sabic) were used as the matrix in the form of films. 10% Maleic Anhydride grafted Polypropylene (MAgPP) was used to enhance the bonding between Kevlar fibre and PP matrix [16]. The importance and schemes of improving the bond strength between Kevlar fibre and matrix materials are well discussed in the literature [24]. Vacuum-assisted compression molding method was used to manufacture composite laminates of Kevlar 129/PP (K-PP) and Kevlar 129/PEI (K-PEI) consisting of 24 layers. The stacking of fabric and matrix sheets was placed in the vacuum assisted compression molding chamber. After closing the molding chamber, a pressure of 10 bar was applied at a temperature of 200 °C for PP and 350 °C for PEI. A vacuum of ~500Hg was implemented to avoid the formation of voids. After completion of the reaction time, laminates were brought to ambient temperature while pressure was maintained.

Laser machining was carried out using a 400W continuous wave fibre laser (Model: RS400, SPI lasers, UK) to produce cylindrical specimens from flat laminates. The diameter of the specimen was kept constant at 11.5 mm, resulting in a theoretical aspect ratio of ~0.42, within experiment tolerance of ±5% error.

Fibre volume fraction (FVF) and density play a substantial role in deciding the mechanical behaviour of composites. The burn-off test was performed for both the K-PP and K-PEI composites as per ASTM D2584. However, simultaneous degradation of Kevlar fibre and PEI matrix didn't allow FVF determination through the burn-off test. Therefore, the thermal decomposition behaviour of the constituent elements was studied using Thermogravimetric analysis (TGA). TGA also helps in understanding the response of the composites under elevated temperature conditions. Accordingly, TGA was performed on the constituent materials i.e. K129 fabric, PP and PEI, as well as, on the K-PP and K-PEI composites, to determine the percentage decomposition as a function of temperature. TGA was performed using Q200 of TA Instruments (Make: New Castle, Delaware USA). The processing parameters used were: (a) rate of heating: 20 °C/min, (b) atmosphere: Nitrogen, (c) temperature range: 50 °C to 850 °C and (d) initial mass of the specimen material: 10–15 mg.

It was observed that PP decomposed completely within the temperature range of 445–505 °C. The primary decomposition temperature range of K129 fibre was observed from 570 to 615 °C. The decomposition temperature of PEI was in the range of 545–600 °C, which is similar to that of K129 fibre (Fig. 1a). From manufacturers datasheets, it is known that PP and PEI attain liquid phase above 200 °C and 350 °C, respectively, at room pressure. Above a temperature of 505 °C, PP

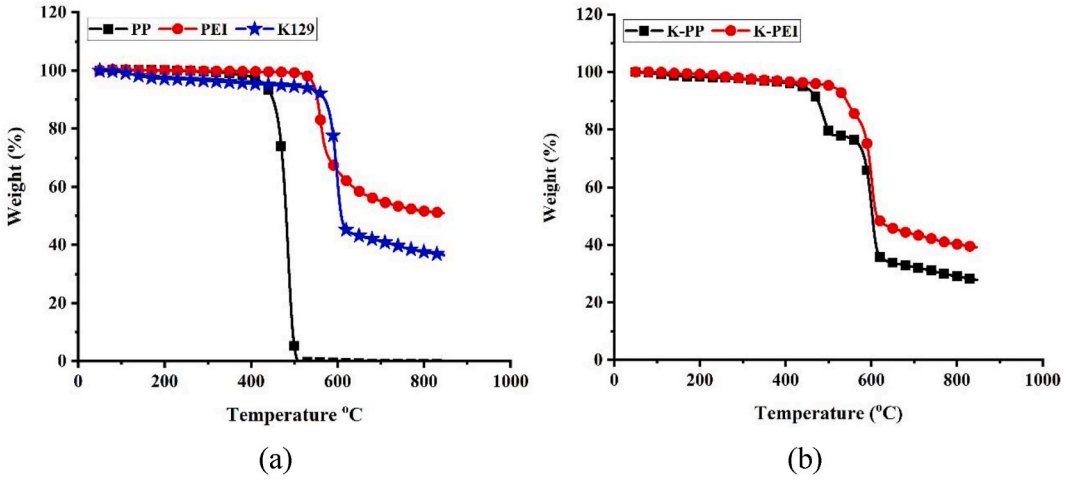

Fig. 1. TGA results: (a) Kevlar-129, PP, PEI and (b) K-PP, K-PEI composites.

decomposed completely. However, PEI retained 50.9% and Kevlar retained 36.5% of its initial mass even at a temperature of 850 °C. This indicates that decomposition of K129 and PEI results in char content when heated to 850 °C. Due to heating, hydrogen and oxygen were removed from the PEI and Kevlar, leaving carbon residue. The existence of char content at elevated temperatures is a good sign, as the presence of matter will leave laminate with some strength as compared to the zero massed ash of PP. Therefore, the use of PEI may be recommended for matrix material if composites are to serve at elevated temperature conditions.

It is evident from the TGA of constituent materials that K-PP composite will result in two distinct zones of weight loss and the same was observed experimentally (Fig. 1b). The first loss of mass depicted in K-PP decomposition was due to the decomposition of the PP matrix. The material left after 505 °C was only K129, which continues to lose the mass until 850 °C. The final weight of K-PP composite was 27.9% of the initial mass. The resulting final weight of K-PEI composite was 39.1% at 850 °C. However, due to the simultaneous decomposition of Kevlar and PEI, the determination of FVF by the burn-off test for K-PEI was not feasible. It may be noted that char content in K-PEI composite was 40% higher than the K-PP composite. Although in the case of K-PP, FVF was determined by the burn-off test, a different technique was required for K-PEI. Therefore, for consistency of results, dissolution by the solvent technique was adopted to determine the FVF of both the composite materials.

Xylene and N, N, Dimethyl Acetamide (DMAc) were used at 80 °C (atmospheric pressure) for 2 hours to dissolve the matrix content of the K-PP and K-PEI composites, respectively. The density and FVF were determined using equations (1) and (2).

$$\rho_c = \frac{m_c}{V_c} \tag{1}$$

m_c is the mass of the composite, V_c is the volume of the composite and ρ_c is the density of the composite.

$$V_f = \frac{W_f/\rho_f}{W_i/\rho_c} \tag{2}$$

where V_f is the FVF, W_i is the initial weight of the composite, W_f is the final weight of fibre left after dissolving matrix, ρ_c is the density of composite and ρ_f is the density of the fibre (1440 kg/m^3). FVF and density of the composites are presented in Table 1.

Table 1
Physical properties of the laminates.

Laminate	No. of layers	Density (kg/m^3)	FVF (%)
K-PP	24	1145	60.70
K-PEI	24	1250	64.85

2.2. Quasi-static and high strain rate tests

Quasi-static testing was performed using a 100 kN Instron Universal Testing Machine (UTM) with a 0.001–500 mm/min speed range and load measurement accuracy of ±0.4%. All the quasi-static compression tests were performed at a constant cross-head speed of 5 mm/min.

High strain rate tests in the compression direction (through-the-thickness) of the specimens were performed using the SHPB apparatus at the Indian Institute of Technology Delhi, India (Fig. 2). This SHPB set-up comprises three Titanium (Ti6Al4V) bars of 16 mm diameter, a striker bar of length 240 mm, an incident bar of length 1200 mm and a transmission bar of length 1200 mm. The titanium bars had a density of ρ = 4430 kg/m^3, Young's modulus of 113.8 GPa and elastic wave speed in the bar material is 5068 m/s. To obtain the adequate dynamic equilibrium in the SHPB test, a pulse shaper having 1.4 mm thickness and 3.1 mm diameter of Linatex (natural rubber) was used between the striker bar and incident bar. The schematic of the SHPB set-up is shown in Fig. 2. A clear discussion on the working of this SHPB setup is explained in detail in the literature [23].

One-dimensional wave propagation in elastic bars with particle motion in longitudinal direction serves as the basis of design for the SHPB test. Complete instrumentation, theory and methodology of SHPB are systemically explained in literature [25,26]. The analytical relations for the determination of specimen strain (ε), strain rates ($\dot{\varepsilon}$) and stress (σ) as a function of time using one-dimensional wave propagation theory are as follows:

$$\varepsilon = \frac{-2C_e}{L_s}\int_0^t \varepsilon_r(t)dt \tag{3}$$

$$\dot{\varepsilon} = \frac{-2C_e}{L_s}\varepsilon_r(t) \tag{4}$$

$$\sigma = \frac{E_b A_b}{A_s}\varepsilon_t(t) \tag{5}$$

where C_e is the wave velocity in the bar material, $\varepsilon_r(t)$ is the reflected strain gauge signal, $\varepsilon_t(t)$ is the transmitted strain gauge signal, L_s is the

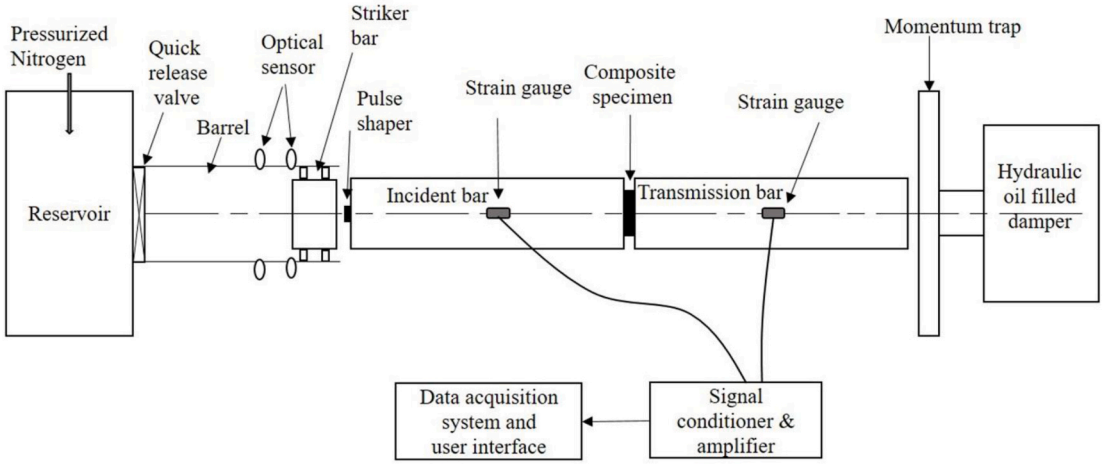

Fig. 2. Schematic SHPB set-up for high strain rate compression tests.

length of the specimen, E_b is the modulus of the bars, A_b is the cross-sectional area of the bar and A_s is the cross-sectional area of the specimen.

For the calculation of the strain rate of homogenous materials, the slope of the strain rate-time curve serves the purpose. However, in the case of the dynamic loading of composites, stress wave attenuation is substantial. Therefore, in this case, the scheme suggested in the literature [27,28] for materials showing stress wave attenuation is used. The strain rate in this work was calculated by dividing the area under the strain rate-strain curve up to maximum strain under loading by the maximum strain.

3. Results and discussion

Quasi-static and high strain rate compression tests were performed on 24 layered K-PP and K-PEI composites. The strain rates varied depending on the constituents of the composites. At least three experiments were conducted to establish the material properties. In this section, the quasi-static and high strain rate compression response of K-PP and K-PEI composites was discussed and compared wherever feasible. From high strain rate response, the limiting strain rate was defined as the strain rate at which an apparent failure was observed in the specimen. The failure of these composites was discussed through digital images and SEM.

3.1. Quasi-static and high strain rate response

Fig. 3 depicts the stress-strain behaviour of K-PP composites under quasi-static and high strain rate loading. Under quasi-static loading, the K-PP specimen exhibited a linear response with no damage up to a strain of 8%. After a strain of 8%, the K-PP specimen followed a non-linear path with a sudden rise in the slope of the curve, indicating initiation of plastic deformation. The primary cause of strain growth at this point was matrix deformation. After 25% of strain, the specimens again showed a linear path, which may be treated as equilibrium in plastic deformation until the peak load is attained. At peak load, the specimen fractures and stress drop instantaneously. The resulting strain rate was calculated as the ratio of peak strain to time.

In the case of high strain rate loading, at strain rates below 4000 s^{-1} K-PP composite resulted in the unloading of the specimen after attaining peak stress. The phenomenon of unloading with a finite strain of 5% in the K-PP specimen indicates an internal failure without the occurrence of notable macroscopic damage. The strain retained by the specimen is an indicator of fibre-matrix debonding and PP matrix damage. It may be noted that at a strain rate of 2548 s^{-1}, a loop in the stress-strain curve was depicted at peak stress in the form of growth in stress with falling

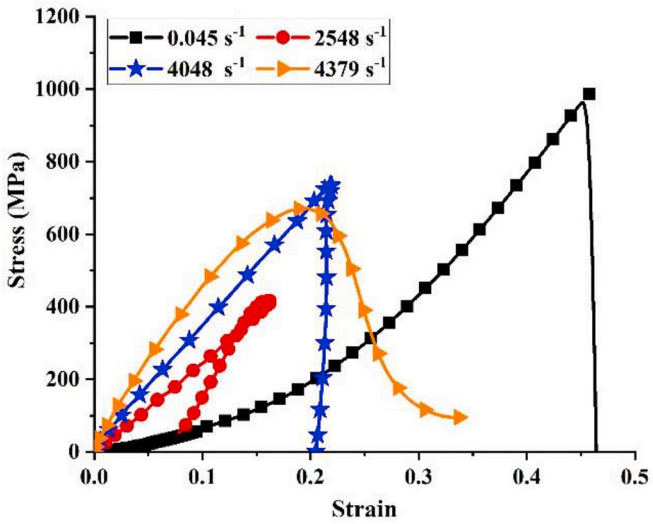

Fig. 3. Quasi-static versus high strain rate response of K-PP.

strain. This unique phenomenon of stress growth with depleting strain was deliberated based on elastic strain energy release as a function of damage. At high strain rates (4048 s^{-1}), an initial linear segment in the stress-strain curve was insignificant, which indicates early attainment of the elastic limit under high strain rates of loading, followed by a non-linear segment. At peak stress, the specimen fractures and the stress diminishes. At a strain rate of 4379 s^{-1} specimens failed catastrophically. The catastrophic failure at the highest loading rate resulted in the enhanced slope of the stress-strain curve, but early damage of specimen resulted in a slight decrement in peak stress. Also, the phenomenon of sudden stress drop at failure was replaced by a gradually diminishing stress curve, as depicted in Fig. 3. The continuous enhancement in the slope of stress-strain curves as a function of rising rates of loading verifies that composite was rate sensitive. These findings are in accordance with the fact that Kevlar fibre [6,7] and thermoplastic (PP) polymer [2,3,15] is highly sensitive to dynamic loading rates.

It may be noted that the peak stress attained in the quasi-static response of the K-PP composite was higher than that of high strain rate loading. The phenomenon of higher stress attainment in the case of quasi-static testing may be attributed to the higher time of test along with peak heat generation at the center of the specimen. At a low (quasi) rate of loading, the matrix gets sufficient time to distribute the generated heat. As a result, the fibres can adjust within the matrix. This

phenomenon of adjustment continues until a few layers or fibre bundles are displaced to produce the delamination effect. At this condition, the UTM detects a sudden change in dimension and the same was recorded as a sudden drop in the load. Whereas, in the case of high strain rate loading, thermal softening takes place due to adiabatic heating. Adiabatic heating, coupled with high strain rate loading results in matrix crushing on the end surfaces. Also, the impedance mismatch between the specimen and incident/transmission bar enhances the damage at the end surface of the specimen. After a limiting condition, the stress wave attains sufficient energy to delaminate Kevlar layers from the transmission side. Hence, the resulting peak stress attained by the specimen was less.

Fig. 4 presents the quasi-static and high strain rate response of K-PEI composites to reveal the difference in behaviour of material due to a change in strain rate. Under quasi-static loading, a linear stress-strain growth was observed until a 10% strain. The linear stress growth was followed by a non-linear growth resulting in plastic deformation up to a strain of ~20%. Further growth in stress was linear in nature, indicating a stable plastic deformation as a function of induced strain until fracture. A minor variation in the quasi-static strain rate for a constant rate cross-head speed of 5 mm/min from 0.045 s^{-1} for K-PP to 0.041 s^{-1} in case K-PEI is due to relatively early brittle fracture of K-PEI.

The high strain rate loading of K-PEI up to 2500 s^{-1} resulted in an intact specimen with stress recovery resulting in a permanent strain of 11–14%. At this strain rate, the failure in the K-PEI was microscopic. For identical loading conditions, K-PP composite experienced permanent strain below 10%, indicating the effect of matrix variation on the composite properties. The limiting strain rate for K-PEI was 3212 s^{-1}, beyond which visible major failure ensues and it was catastrophic in nature. The peak stress increased with an increase in the strain rate up to a threshold and beyond this threshold, peak stress decreased.

Further higher loading rates resulted in the identical higher slope of stress growth. The peak stress decreased at a strain rate of 4274 s^{-1}, due to early brittle failure of the specimen and this brittle nature of PEI matrix completely varied with the rate-dependent phenomenon of the composite. When compared to quasi-static test results, the dynamic K-PEI properties were higher. Higher stresses under dynamic load conditions were attributed to lack of time for damage growth in case of dynamic load conditions as compared to quasi-static loading conditions. Though Kevlar yarns were present in the K-PEI specimen, the PEI matrix dominated the failure mechanisms by undergoing brittle failure.

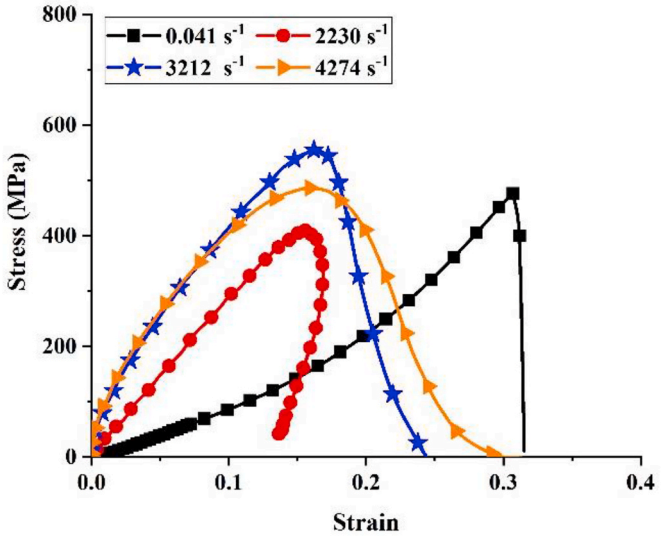

Fig. 4. Quasi-static versus high strain rate response of K-PEI.

3.2. Failure analysis

Failure analysis was performed macroscopically and microscopically. The macroscopic analysis was carried out by taking digital images of the specimens as soon as the test was completed. Microscopic analysis was performed by assessing failed images using scanning electron microscopy (SEM).

3.2.1. Macroscopic analysis

Fig. 5 shows the macroscopic damage of K-PP composites under quasi-static and high strain rate loading conditions and the damage patterns were significantly different. In the case of high strain rates, at a strain rate of 2548 s^{-1} (below-limiting strain rate), unloading of stress indicated macroscopically insignificant damage and the specimen was intact without any significant visible damage. The only failure observed was through matrix crushing and fibre-matrix debonding (Fig. 5a). At limiting strain rate (4048 s^{-1}), the surface in contact with incident bar (front face) (Fig. 5b) suffered matrix crush while the surface in contact with transmission bar (back face) (Fig. 5c) was damaged due to release of few Kevlar layers and some fibres stuck to the free surface. This type of failure indicates the delamination as a primary mode of failure of the K-PP composite. At a strain rate of 4379 s^{-1}, the matrix was no more capable of holding the fibres and the fibres started squeezing out at multiple locations resulting in delamination and fibre pull-out at multiple locations (Fig. 5d).

Fig. 5e depicts the view of the K-PP specimen under quasi-static loading. It was observed that the top and bottom surfaces in contact with platens of UTM were insignificantly damaged and Kevlar fibres were busted out from the center of the specimen (Fig. 5e). It may be noted that in the case of a high strain rate of loading, the total loading time was less than 150 μs, while in quasi-static loading, the same was above 10 sec. Due to the availability of sufficient time for adjustment of fibre and matrix, the quasi-static test resulted in the sliding of Kevlar layers from the center of the specimen as depicted in Fig. 5e. To check the state of the specimen at the center, the specimen was opened manually (Fig. 5f). Matrix free irregular surface with the minor inclined plane was observed; however, the angle could not be measured due to the irregularity and fibrous surface. This may be attributed to the viscous nature of the PP matrix. Due to compressive loading, the heat generated inside the specimen permitted the fibres to squeeze out from the viscous PP matrix.

Fig. 6 shows the damage patterns of K-PEI composite under quasi-static and high strain rate loading conditions and these patterns were significantly different. Besides, the damage patterns were entirely different as compared to the K-PP composite. Irrespective of the type of loading, K-PEI composite behaved in a brittle manner, resulting in distinct shear failure. In the case of a high strain rate, at a strain rate of 2230 s^{-1} (Fig. 6a), the specimen was intact and the failure was microscopic. The fibrous sheared surface clearly indicates a distinct shear plane (Fig. 6b), when the specimen was loaded at 3212 s^{-1} strain rate.

Further higher strain rates resulted in multiple damaged pieces. The difference of failure in K-PEI and K-PP specimens was damaged/dislodged in the former case, while the latter case resulted in delamination on the transmission side of the specimen at higher strain rates. In the case of quasi-static loading, the double-sided brittle fracture was observed. The resulting specimen after the quasi-static test was broken down into three distinct pieces, as shown in Fig. 6d. The shear plane for K-PEI specimens loaded under high strain rate and quasi-static loading was in the range of 30°–50°. However, most of the specimens undergoing brittle damage and resulted in a distinct single shear plane with a shear plane angle of 40°–45°. A precise value of shear plane angle cannot be claimed due to the fibrous surface after specimen failure. The variation in shear plane angles is attributed to the rate of loading and minor difference in the composition/microscopic defects of an individual specimen.

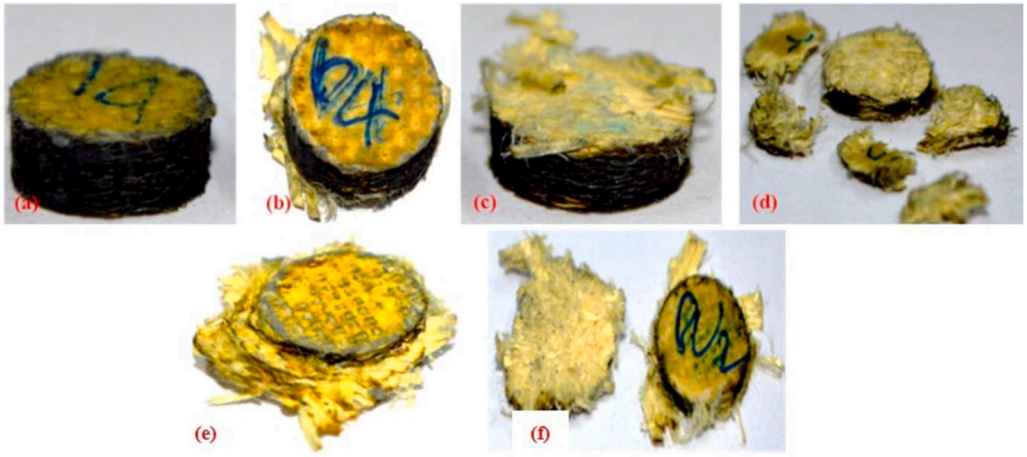

Fig. 5. Macroscopic failure of K-PP composites: (a) 2548 s^{-1}, (b) 4048 s^{-1} (incident side), (c) 4048 s^{-1} (transmission side), (d) 4379 s^{-1}, (e) quasi-static damage (intermediate layers) and (f) quasi-static (opened two sides of specimen).

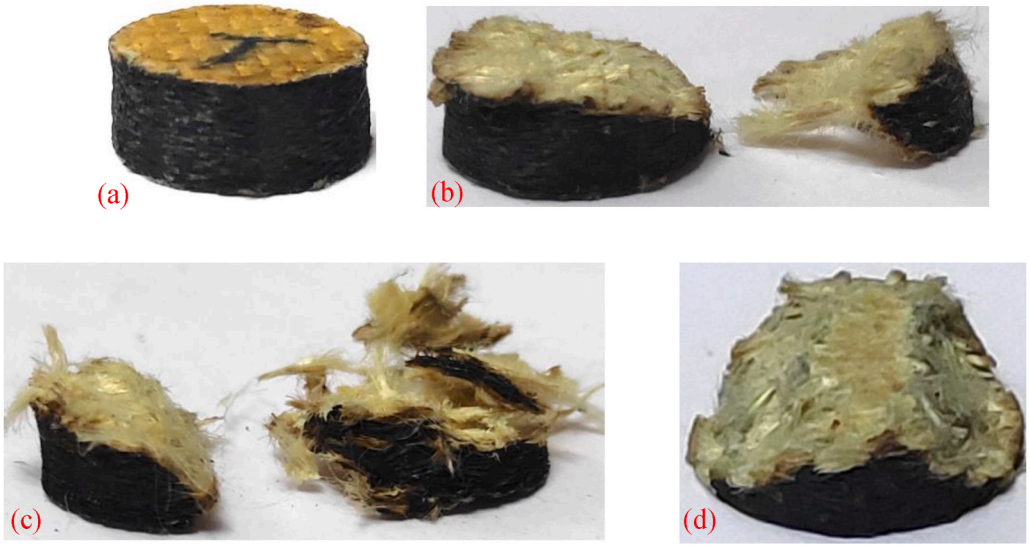

Fig. 6. Macroscopic failure of K-PEI composites: (a) 2230 s^{-1}, (b) 3212 s^{-1}, (c) 4274 s^{-1} and (d) Quasi-static.

3.2.2. *Fractography*

Fig. 7 shows SEM micrographs of the K-PP specimen impacted at a strain rate of 2548 s^{-1}. The specimen may be divided into three distinct zones for a better understanding of the damage pattern. The microscopic failure primarily consisted of crushing, cracking, and fracture of the matrix with fibre-matrix debonding, fibre pull-out and local delamination. The surface in contact with the incident bar receives the impact and stress wave travels through the specimen with several internal fibre–matrix failure in the form of de-bonding (Fig. 7a), resulting into the rise in the reflection voltage well before transmission signal rise.

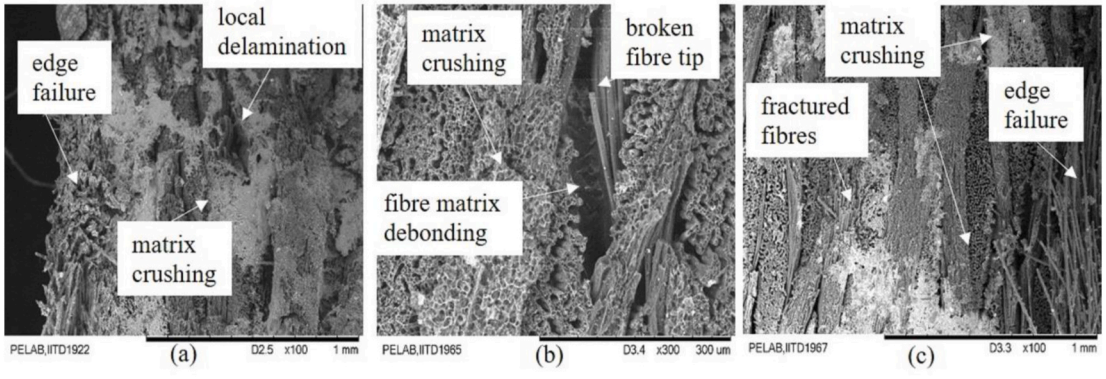

Fig. 7. SEM micrographs of K-PP at 2548 s^{-1}: (a) incident bar side (b) mid of specimen and (c) transmission bar side.

Edge failure was an outcome of dislodging of the matrix in the powder form from the composite specimen as a function of the incident stress wave. Matrix crushing resulted in fibre exposure on the end surfaces of the specimen. Matrix cracking, shear and crushing induced void formation and local delamination were primary failure modes at mid-section of the entire specimen (Fig. 7b). Fibre fracture was confirmed by the presence of broken fibre ends. On the transmission bar side of the specimen, severe damage was depicted. Fibre fracture, matrix crushing and delamination were depicted in Fig. 7c.

Fig. 8 shows the SEM micrographs of K-PEI specimen at higher strain rates. At a strain rate of 2230 s^{-1}, no significant failure was observed through SEM. Beyond this strain rate, the K-PEI specimen failed into pieces due to the brittle nature. Therefore, SEM micrographs of these specimens at the impact side are shown. At higher strain rates, specimen macroscopically disintegrated into multiple failed pieces due to multiple brittle cracks induced shear planes. As an outcome, multiple bundles of failed fibres, broken fibres along with disintegrated matrix lump were noticeable (Fig. 8a). At few locations, fibre matrix shear plane is visible due to shear crack propagation (Fig. 8b). Also, shear failure of the matrix along with fibre within a lamina were noted. At a few rare locations, fibre thinning was also depicted (Fig. 8b), indicating the resistance offered by Kevlar fibre due to which a consistent shear plane is not witnessed. All the failure modes were majorly due to the brittle nature of the PEI matrix and this shear failure was consistent with the macroscopic images observed. Similar damage phenomenon resulting in matrix damage induced delamination followed by fibre failure has been reported in the literature for both, the HSR testing [17,18,20] and for projectile impact [29].

3.3. Comparison of quasi-static and high strain rate response between K-PP and K-PEI

Under quasi-static and high strain rate loading conditions, K-PP exhibited a ductile response while for K-PEI it was brittle. Under quasi-static loading, the maximum stress of K-PP composite was higher as compared to the peak stress obtained at limiting high strain rates. However, in the case of K-PEI, the maximum stress under quasi-static loading was lower than the limiting strain rate of loading. This may be attributed to the brittle nature of K-PEI composite. At high strain rates, after unloading, at a strain rate of 2230 s^{-1}, the permanent strain induced in K-PEI specimen was above 10% and for K-PP it was less than 10% at a strain rate of 2548 s^{-1}. Another important point of difference between K-PP and K-PEI composite was in peak strain rate acquired. K-PP attained the highest strain rate as compared to the K-PEI under identical loading conditions. This difference in properties for Kevlar129 fibre-based composite was attributed to change in the deformation and damage behaviour of matrix material. Table 2 depicts the stress and strain attained by K-PP and K-PEI specimen under quasi-static and high strain rate loading. It can be observed that the K-PP composite exhibited better performance as compared to the K-PEI composites.

Fig. 9 shows the comparison of high stain rate properties between K-PP and K-PEI composites. The high strain rate results of K-PP and K-PEI revealed a significant difference in strain rates and dynamic compressive properties. An important point of concern is the effect of specimen aspect ratio. For both the composites, the specimen dimensions resulting in an ideal aspect ratio revealed the highest stresses. The limiting strain rate at which physical damage ensues for K-PP was 4048 s^{-1} while for K-PEI it was 3212 s^{-1}. At limiting strain rate, K-PP attained 25%, 27% and 6% higher peak stress, peak strain and toughness as compared to the K-PEI composite, respectively. Also, the properties of K-PP were compared with the Kevlar 29 reinforced PP composites (K29-PP) reported in the literature [15].

The strain rates reported in Ref. [15] were 2538 s^{-1}, 3239 s^{-1} and 4264 s^{-1}, which were close to the strain rates obtained for K-PP in the present study. High strain rate properties of present K-PP were 3–12% and 38–54% higher in terms of peak stress and peak strain, respectively, as compared with that of K29-PP [15]. The toughness of K-PP of the present study was less at lower strain rates as compared to that of K29-PP [15]. However, toughness enhanced over K29-PP with an increase in the rate of loading. Table 3 shows the high strain rate properties of K-PP and K-PEI composites.

4. Conclusions

In the present study, a comparative study on the quasi-static and high strain rate response of K-PP and K-PEI composites was carried out. Quasi-static testing of K-PP composite revealed that it's primarily the viscous nature of PP matrix, which permits sliding of Kevlar layers as a function of the rate of loading and number of layers. This behaviour changes from sliding of middle layers to delamination of end layers while moving from quasi-static to high strain rate loading. Also,

Table 2
Quasi-static and limiting strain rate properties of K-PP and K-PEI.

Type of laminate	K-PP	K-PEI
Quasi-static peak stress (MPa)	986 ± 47	460 ± 23
Quasi-static peak strain (%)	46 ± 2.2	29 ± 1.6
Dynamic peak stress at limiting condition (MPa)	738 ± 36	447 ± 21
Dynamic peak strain (%)	22 ± 1.4	23 ± 1.5

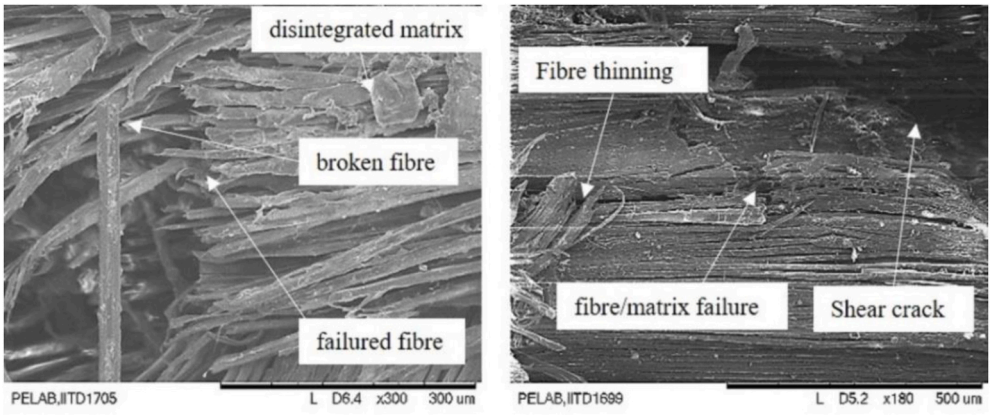

Fig. 8. SEM micrographs of K-PEI at 3212 s^{-1}.

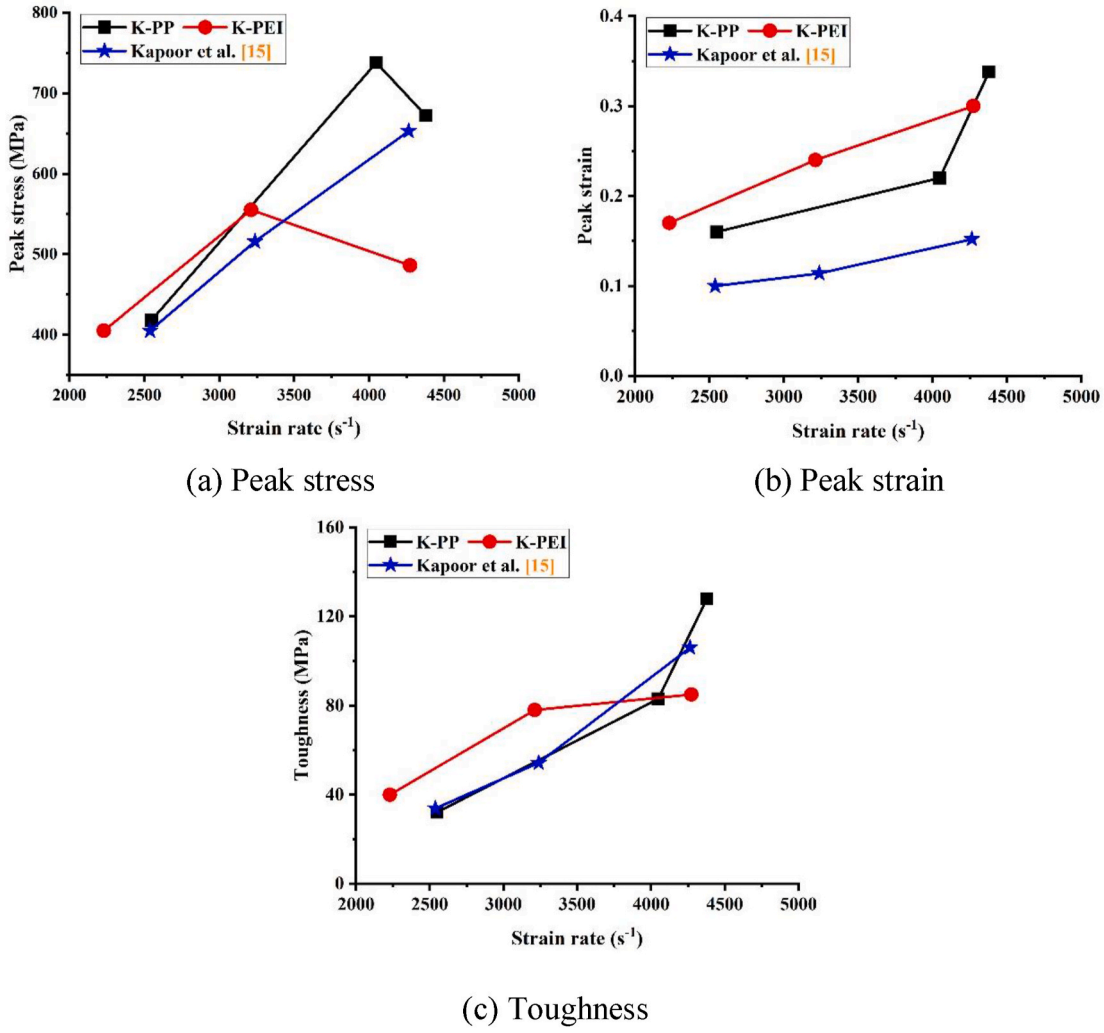

Fig. 9. Comparison of high strain rate properties.

Table 3
High strain rate properties of K-PP and K-PEI.

Composite	Strain rate (s^{-1})	Peak strain	Peak stress (MPa)	Toughness (MPa)
K-PP	2548	0.16	418	32
	4048	0.22	738	83
	4379	0.33	672	128
K-PEI	2230	0.17	405	40
	3212	0.24	555	78
	4274	0.30	486	85
K29-PP [15]	2538	0.10	405	34
	3239	0.11	516	54
	4264	0.15	653	106

dynamic loading permits fibre pull-out and matrix crushing, a phenomenon missed during quasi-static testing of K-PP composite. K-PEI, on the other hand, revealed the brittle composite fracture. Based on the present work following conclusions were drawn;

(i) The compressive properties enhance with increasing strain rates of loading for K129 composites under high strain rate regime. However, it may not be possible while switching from quasi-static to high strain rate loading.
(ii) Interestingly, K-PP composite under quasi-static loading could perform better compared to dynamic loading for identical specimen dimensions. The peak stress of K-PP under quasi-static test was 33–47% higher than the dynamic test results. In the case of K-PEI, the results were opposite to K-PP test results.
(iii) High strain rate properties of K-PP of the present study were 3–12% and 38–54% higher than that of K29-PP composites in terms of peak stress and peak strain, respectively. K-PP of the present study is better than K29-PP for the high strain rate conditions.
(iv) With the increasing rate of loading, the composite properties enhance until limiting strain rate of loading, after which properties start depleting.
(v) PP is capable of allowing fibre deformation and fibre pull-out under compression, whereas PEI matrix-based composites suffer brittle fracture without allowing fibre movement.
(vi) Kevlar-thermoplastic composites can be tailored as energy-absorbing or dissipating material systems by varying the thermoplastic matrix material from PP to PEI.

CRediT authorship contribution statement

Hemant Chouhan: Conceptualization, Methodology, Formal analysis, Resources, Investigation, Data curation, Validation, Writing - original draft, Writing - review & editing. **Neelanchali Asija Bhalla:** Conceptualization, Methodology, Formal analysis, Resources, Investigation, Data curation, Validation. **Aswani Kumar Bandaru:** Investigation, Formal analysis, Data curation, Writing - review & editing. **Shishay Amare Gebremeskel:** Methodology, Investigation, Data curation,

Validation. **Naresh Bhatnagar:** Conceptualization, Resources, Investigation, Supervision, Writing - review & editing, Project administration.

Declaration of competing interest

The authors declare that they have no known competing financial interests or personal relationships that could have appeared to influence the work reported in this paper.

Acknowledgment

The authors are indebted to IRD-IITD for a grand challenge grant (MI00810) for this research project.

References

[1] B. Sun, B. Gu, X. Ding, Compressive Behavior of 3-D Angle-Interlock Woven Fabric Composites at Various Strain Rates, vol. 24, 2005, pp. 447–454, https://doi.org/10.1016/j.polymertesting.2005.01.005.
[2] K. Nakai, T. Yokoyama, Uniaxial compressive response and constitutive modeling of selected polymers over a wide range of strain rates, J. Dyn. Behav. Mater. 1 (2015) 15–27.
[3] M. Firdaus, H. Akil, Z. Arifin, Measurement and prediction of compressive properties of polymers at high strain rate loading, Mater. Des. 32 (2011) 4207–4215, https://doi.org/10.1016/j.matdes.2011.04.037.
[4] N.J. Mutter, Characterization of dynamic and static mechanical behavior of Polyetherimide, Dep. Mech. Mater. Aerosp. Eng. MSc Thesis (2012) 11–13, internal-pdf://0928946789/Mutter_2012_XX_B_thesis PEI.pdf.
[5] J. Lim, W.W. Chen, J.Q. Zheng, Dynamic small strain measurements of Kevlar 129 single fibers with a miniaturized tension Kolsky bar, Polym. Test. 29 (2010) 701–705, https://doi.org/10.1016/j.polymertesting.2010.05.012.
[6] V.B.C.Ã. Tan, X.S. Zeng, V.P.W. Shim, Characterization and Constitutive Modeling of Aramid Fibers at High Strain Rates, vol. 35, 2008, pp. 1303–1313, https://doi.org/10.1016/j.ijimpeng.2007.07.010.
[7] T.J. Singh, S. Samanta, Characterization of kevlar fiber and its composites: a review, Mater. Today Proc. 2 (2015) 1381–1387, https://doi.org/10.1016/j.matpr.2015.07.057.
[8] D. Zhu, B. Mobasher, A. Vaidya, S.D. Rajan, Mechanical behaviors of Kevlar 49 fabric subjected to uniaxial, biaxial tension and in-plane large shear deformation, Compos. Sci. Technol. 74 (2013) 121–130.
[9] Y. Wang, Y. Xia, The effects of strain rate on the mechanical behaviour of kevlar fibre bundles: an experimental and theoretical study, Compos. Part A. 29 A (1998) 1411–1415.
[10] Y. Ou, D. Zhu, H. Zhang, L. Huang, Y. Yao, G. Li, B. Mobasher, Mechanical characterization of the tensile properties of glass fiber and its reinforced polymer (GFRP) composite under varying strain rates and temperatures, Polymers 8 (2016) 1–16, https://doi.org/10.3390/polym8050196.
[11] X. Zhang, D. Zhu, Y. Yao, H. Zhang, B. Mobasher, L. Huang, Experimental study of tensile behaviour of AFRP under different strain rates and temperatures, J. Struct. Integr. Maint. 1 (2016) 22–34, https://doi.org/10.1080/24705314.2016.1153327.
[12] Y. Ou, D. Zhu, Tensile behavior of glass fiber reinforced composite at different strain rates and temperatures, Constr. Build. Mater. 96 (2015) 648–656, https://doi.org/10.1016/j.conbuildmat.2015.08.044.
[13] Y. Ou, D. Zhu, H. Li, Strain rate and temperature effects on the dynamic tensile behaviors of glass and basalt fiber reinforced polymer composites, J Mater. Civ. Enginering. (2016) 1–10, https://doi.org/10.1061/(ASCE)MT.1943-5533.0001615, 04016101.
[14] S.C. Woo, T.W. Kim, High-strain-rate impact in Kevlar-woven composites and fracture analysis using acoustic emission, Compos. Part B Eng. 60 (2014) 125–136, https://doi.org/10.1016/j.compositesb.2013.12.054.
[15] S. Woo, T. Kim, High strain-rate failure in carbon/Kevlar hybrid woven composites via a novel SHPB-AE coupled test, Compos. Part B. 97 (2016) 317–328, https://doi.org/10.1016/j.compositesb.2016.04.084.
[16] B. Viswanathan, J.R. Vinson, B.R. Scott, High strian rate compression testing of Kevlar29/Polyethylene composite with very high fiber volume fraction, Am. Inst. Aeronaut. Astronaut. Inc. A98–25136 (1998) 1342–1352.
[17] K. Shaker, A. Jabbar, M. Karahan, N. Karahan, Y. Nawab, Study of dynamic compressive behaviour of aramid and ultrahigh molecular weight polyethylene composites using Split Hopkinson Pressure Bar, J. Compos. Mater. 51 (2017) 81–94, https://doi.org/10.1177/0021998316635241.
[18] J. Zhao, L. Zhang, L. Guo, Y. Yang, Dynamic properties and strain rate effect of 3D angle-interlock carbon/epoxy woven composites, J. Reinf. Plast. Compos. 36 (2017) 1531–1541, https://doi.org/10.1177/0731684417715712.
[19] B. Song, W. Chen, T. Weerasooriya, Quasi-static and dynamic compressive behaviors of a S-2 glass/SC15 composite, jr, Compos. Mater. 37 (2003) 1723–1744.
[20] R. Kapoor, L. Pangeni, A.K. Bandaru, S. Ahmad, N. Bhatnagar, High strain rate compression response of woven Kevlar reinforced polypropylene composites, Compos. Part B. 89 (2016) 374–382, https://doi.org/10.1016/j.compositesb.2015.11.044.
[21] E.D.H. Davies, S.C. Hunter, The dynamic compression test of solids by the method of the split Hopkinson pressure bar, J. Mech. Phys. Solids. 11 (1963) 155–179.
[22] A.K. Bandaru, V.V. Chavan, S. Ahmad, R. Alagirusamy, N. Bhatnagar, Ballistic impact response of Kevlar® reinforced thermoplastic composite armors, Int. J. Impact Eng. 89 (2016) 1–13, https://doi.org/10.1016/j.ijimpeng.2015.10.014.
[23] A.K. Bandaru, H. Chouhan, N. Bhatnagar, High strain rate compression testing of intra-ply and inter-ply hybrid thermoplastic composites reinforced with Kevlar/basalt fibers, Polym. Test. 84 (2020) 106407, https://doi.org/10.1016/j.polymertesting.2020.106407.
[24] L. Luo, Y. Yuan, Y. Dai, Z. Cheng, X. Wang, X. Liu, The novel high performance aramid fibers containing benzimidazole moieties and chloride substitutions, Mater. Des. 158 (2018) 127–135, https://doi.org/10.1016/j.matdes.2018.08.025.
[25] M.V. Hosur, J. Alexander, U.K. Vaidya, S. Jeelani, High strain rate compression response of carbon/epoxy laminate composites, Compos. Struct. 52 (2001) 405–417.
[26] M. Firdaus, H. Akil, Z. Arifin, Static and dynamic compressive properties of mica/polypropylene composites, Mater. Sci. Eng. A. 528 (2011) 1567–1576, https://doi.org/10.1016/j.msea.2010.10.071.
[27] K. Nakai, T. Yokoyama, Strain rate dependence of compressive stress-strain loops of several polymers, J. Solid Mech. Mater. Eng. 2 (2008) 557–566, https://doi.org/10.1299/jmmp.2.557.
[28] T. Yokoyama, K. Nakai, Determination of the impact tensile strength of structural adhesive butt joints with a modified split Hopkinson pressure bar, Int. J. Adhes. Adhes. 56 (2015) 13–23. http://linkinghub.elsevier.com/retrieve/pii/S014374961400150X.
[29] W. Ferreira, D.A. Junior, R. Carla, S. Felipe, L.B. Neto, R. Carlos, S. Freire, The variation in low speed impact strength on glass fiber/Kevlar composite hybrids, Jr Compos. Mater. (2020) 1–11, https://doi.org/10.1177/0021998320906205.
[30] Hemant Chouhan, Neelanchali Asija Bhalla, Naresh Bhatnagar, High strain rate performance of UHMWPE composites: Effect of moisture ingress and egress, Materialstoday Communications (2020), 101709, https://doi.org/10.1016/j.mtcomm.2020.101709. In press.